RESEARCH ARTICLE | SEPTEMBER 02 2020

Introduction to lateral resolution and analysis area measurements in XPS

Special Collection: Special Topic Collection: Reproducibility Challenges and Solutions

Wolfgang E. S. Unger ; Jörg M. Stockmann; Mathias Senoner; Thomas Weimann; Sebastian Bütefisch; Cristiana Passiu; Nicholas D. Spencer; Antonella Rossi

Journal of Vacuum Science & Technology A 38, 053206 (2020)
https://doi.org/10.1116/6.0000398

JVST A
Journal of Vacuum Science & Technology A

ARTICLE

avs.scitation.org/journal/jva

Introduction to lateral resolution and analysis area measurements in XPS

Cite as: J. Vac. Sci. Technol. A **38**, 053206 (2020); doi: 10.1116/6.0000398
Submitted: 12 June 2020 · Accepted: 27 July 2020 ·
Published Online: 2 September 2020

Wolfgang E. S. Unger,[1,a)] Jörg M. Stockmann,[1] Mathias Senoner,[1] Thomas Weimann,[2] Sebastian Bütefisch,[2] Cristiana Passiu,[3] Nicholas D. Spencer,[3] and Antonella Rossi[3,4,b)]

AFFILIATIONS

[1]Bundesanstalt für Materialforschung und -prüfung (BAM), 12200 Berlin, Germany
[2]Physikalisch-Technische Bundesanstalt (PTB), 38116 Braunschweig, Germany
[3]Laboratory for Surface Science and Technology, Department of Materials, ETH Zurich, Vladimir-Prelog-Weg 5, CH-8093 Zürich, Switzerland
[4]Dipartimento di Scienze Chimiche e Geologiche, Università di Cagliari, Monserrato, 09142 Cagliari, Italy

Note: This paper is part of the Special Topic Collection on Reproducibility Challenges and Solutions.
[a)]**Electronic mail:** wolfgang.unger@alumni.hu-berlin.de
[b)]**Electronic addresses:** antonella.rossi@mat.ethz.ch and rossi@unica.it

ABSTRACT

Imaging and small-spot (small area) XPS have become increasingly important components of surface chemical analysis during the last three decades, and its use is growing. Some ambiguity in the use of terminology, understanding of concepts, and lack of appropriate reference materials leads to confusing and not always reproducible data. In this paper, it is shown that by using existing knowledge, appropriate test specimens, and standardized approaches, problems of comparability and such reproducibility issues recently observed for XPS data reported in the scientific literature can be overcome. The standardized methods of ISO 18516:2019, (i) the straight-edge, (ii) the narrow-line, and (iii) the grating method, can be used to characterize and compare the lateral resolution achieved by imaging XPS instruments and are described by reporting examples. The respective measurements are made using new test specimens. When running an XPS instrument in the small-spot (small area) mode for a quantitative analysis of a feature of interest, the question arises as to what contribution to the intensity originates from outside the analysis area. A valid measurement approach to control the intensity from outside the nominal analysis area is also described. As always, the relevant resolution depends on the specific question that needs to be addressed. The strengths and limitations of methods defining resolution are indicated.

I. INTRODUCTION

Imaging and small-spot (small area) XPS became very important methods in surface chemical analysis during the last three decades. The approach is widely applied in testing laboratories in industry and academia. Depending on the analysis question or objective, it is useful to know both the nature of the resolution of measurements in the instrument used and how the relevant data are collected and analyzed. In some circumstances, it is useful to distinguish between features and dominant composition in different regions of a sample. The resolution needed to distinguish major regions can be quite different than the requirements to obtain the detailed chemical composition and the possibility of contamination of nearby species in a specific region of a sample. Thus, it is important to understand relevant concepts of resolution, the nature of the instrument, and how both relate to the analysis question. This guide introduces three methods commonly used for identifying instrument resolution, notes their strengths and limitations, and points to the relationship of the straight-edge method to small area analysis.

There are many XPS instruments sold worldwide, and many of these instruments show ultimate performance in imaging and small area analysis. The industry uses imaging and small-spot XPS as they get results that are good, helpful, and underpin product development. In spite of this, the authors of Refs. 1 and 2 identified

a general problem in XPS analysis "… that in many publications where XPS use is reported, the information is limited in some way and that too often the XPS data reported are incomplete or misinterpreted …." Of course, that problem also occurs in applications of small area or imaging XPS. That valid opinion points to the fact that there is a need for improvement, specifically in comparability and reproducibility of XPS data reported. Therefore, the editorial board of JVST with support by the AVS decided to launch the preparation of a *Special Topic Collection: Reproducibility Challenges and Solutions* with a focus on XPS measurements. With a specific view on imaging and small-spot XPS, it will be demonstrated in this paper that problems of comparability and reproducibility can be substantially reduced by using existing resources.

Basically, when applying imaging surface chemical analysis, an analyst wishes to determine the local chemical surface composition of some identified region of interest. There is an increasing need to characterize devices with dimensions on the micrometer scale using analysis tools with lateral resolutions that are smaller than those of the features of interest. The aim of such characterization is to determine that devices have been fabricated as intended to evaluate new or current fabrication methods and to identify failure mechanisms of a device during its life cycle. There are many applications published so far. Here, we refer to an example from tribology where XPS was used to discriminate between the chemical composition of micrometer-scaled contact and noncontact areas on the surfaces of tribo-pairs.[3,4]

The two principal analytical tasks enabled by XPS are (i) to analyze the integral chemical composition of a micrometer-scaled feature on a sample surface and (ii) to take a chemical map covering a feature of interest with micrometer dimensions. To achieve comparability and reproducibility, the analysis area addressed in small-spot XPS and the lateral resolution of an imaging XPS instrument are very important parameters to be determined in a proper way. To reach that goal, application of standardized measurement procedures is recommended. Moreover, the use of a consistent terminology in scientific publications is also mandatory to avoid misunderstanding, confusion, and erroneous results. The authors of Ref. 5 comprehensively introduced the agreed terminology related to *lateral resolution* and *analysis area* in the JVST *Special Topic Collection: Reproducibility Challenges and Solutions*.

The determination of lateral resolution in XPS (and AES and SIMS as well) is introduced in the Technical Report ISO/TR 19319:2013 (Refs. 6 and 7) and methods standardized in ISO 18516:2019.[8,9] The 90-page long Technical Report introduces models of image formation and explains the meanings of point spread function (PSF), line spread function (LSF), and edge spread function (ESF) in the given context. Lateral resolution is discussed as a property of an image produced by an (XPS) instrument at specific operation parameters. It is shown in the Technical Report that the noise level achieved in the image has also impact on the lateral resolution (cf. Ref. 10). Finally, recommendations for the design of appropriate test specimen are given, and the uncertainty of a measurement of the lateral resolution is considered in the Technical Report as well.

The determination of the analysis area is addressed in ASTM E1217-11 (Ref. 11) and Refs. 5 and 12.

Because of the increasing importance of XPS imaging and small area analysis, approaches for the determination of instrumental performance parameters such as lateral resolution and analysis area were recently tested and evaluated by international experts participating in interlaboratory comparisons under the umbrella of the VAMAS TWA2 Project A22. New test specimens[13] were used, and proposals for their optimization were elaborated during the project. VAMAS TWA2 *Surface Chemical Analysis* regularly reports the results of A22 to the subcommittee SC7 *Electron Spectroscopies* of ISO TC 201 *Surface Chemical Analysis*. The results of A22 will lead to the development of a new ISO standard on the determination of the intensity from outside the analysis area of an XPS instrument used in the small-spot analysis mode.

For more details on the process of standardization and the acting parties, see Ref. 14.

II. MEASUREMENT OF LATERAL RESOLUTION IN IMAGING XPS

A. Background

In imaging XPS, a feature of interest is generally analyzed by using a full image or line-scans in which a selected photoelectron signal is displayed as a function of position on the sample surface. This approach is often also called "mapping." The detectability of a feature of a specific dimension requires instrumental operation parameters, which enable the lateral resolution needed. Of course, a material contrast (seen by the XPS method) between the feature and its surroundings on the analyzed surface and an appropriately low noise level in the image or line-scans acquired are necessary as well.

In the terminology standard ISO 18115-1, *lateral resolution* (term 4.385) is defined as a "distance, …, over which changes in composition can be separately established with confidence" (cf. Ref. 5). This definition for itself does not tell anything about a practical implementation and is, therefore, complemented by a note where reference is made to the use of a small emitting point for a determination of the PSF and to the straight-edge method, both enabling a measurement of the lateral resolution. A common understanding of the lateral resolution in other communities of microscopy (e.g., that related to electron microscopy) is that it is "the minimum spacing at which two features of an image can be recognized as distinct and separate."[15] Lateral resolution in XPS is also referred to as spatial resolution.

Because lateral resolution is discussed in this paper using terms of the theory of image formation, i.e., PSF, LSF, and ESF, a brief introduction of what is behind seems to be useful at this point. For a more complete description, see Clauses 4.1.1, 4.1.2, and 4.1.3 in ISO/TR 19319:2013.

The imaging process describes the formation of an image as a result of the interaction between an object and an imaging system (cf. Fig. 1). In imaging XPS, the object is represented by the object pattern established as a distribution of a certain parameter, for instance, a surface concentration of an element (e.g., carbon) or a chemical species (e.g., carbon in a carboxyl group). The imaging process transfers this distribution to a respective signal intensity distribution measured by the instrument. The imaging instrument is represented by its PSF. The PSF is the normalized 2D distribution of signal intensity in the image of an infinitely small point being the imaged object. The LSF is the normalized intensity distribution in the image of an infinitely narrow line, the object pattern.

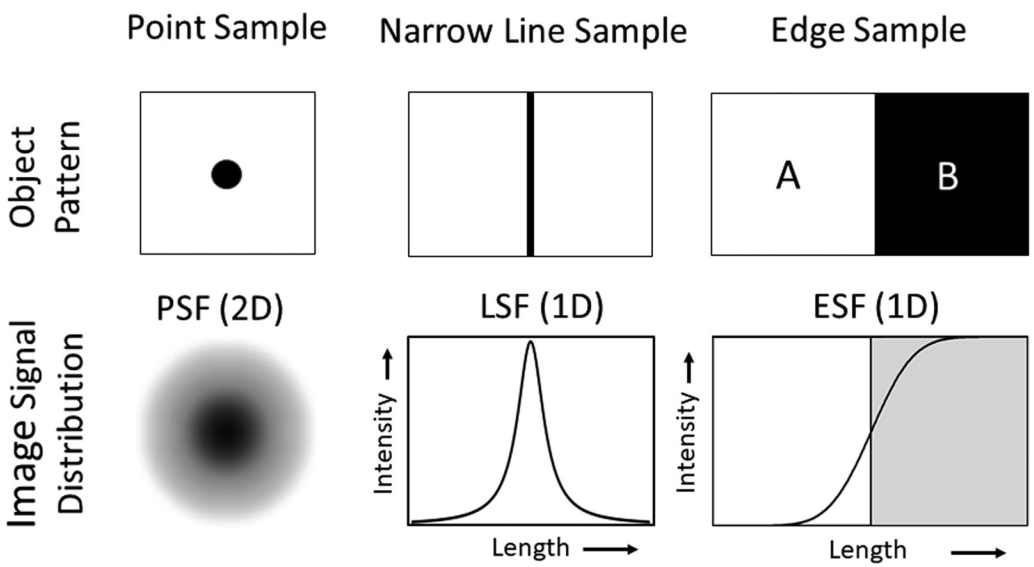

FIG. 1. Different object patterns (infinitely small point, narrow line, and sharp edge) and the related signal distributions measured by the imaging instrument. Material A is shown white and material B in black. These signal distributions are named PSF, LSF, and ESF. LSF and ESF are usually presented as one-dimensional line-scans across the respective signal distributions.

It can be viewed as a superposition of many PSFs related to infinitely small points organized along a line in the object pattern. Typically, the LSF is presented as a (one-dimensional) line-scan across the normalized intensity distribution. The ESF is the normalized distribution of signal intensity in the image of an infinitely sharp edge (step transition), also presented as a one-dimensional line-scan across the normalized intensity distribution. The ESF is the integral of the LSF. ISO/TR 19319:2013 reports simulations visualizing the substantial impact of the shape of the LSF, expressed as Gaussian, Lorentzian, or Pseudo-Voigt (50% weights) functions, on the shape of the ESF and the derived $D_{x\text{-}(100-x)}$ parameter used to characterize the lateral resolution (cf. Fig. 12 in Clause 4.2 and Figs. 32 and 33 in Clause 4.3 of Ref. 6).

There are two approaches to design instruments enabling imaging XPS. The first setup uses a focused incident x-ray beam delivered by an x-ray monochromator and raster scanned across the sample's surface and an electron energy analyzer system accepting all the photoelectrons emitted from the raster scanned area. X-ray beams characterized by their diameters below 10 μm expressed as a full width at half maximum (FWHM) are available. In the case the angle of incidence of the x-ray beam is larger than 0° (normal incidence), the footprint of the x-ray beam becomes elliptic and the lateral resolution depends on the azimuth angle.[6,8]

The second design uses larger x-ray spots that are nowadays delivered by a monochromator. Imaging is achieved by using a stack of magnetic and electrostatic lenses with low spherical aberrations to project a magnified image of the surface feature of interest onto the entrance plane of an electron energy analyzer (e.g., a spherical mirror analyzer). An energy filtered subset of the photoelectrons is transmitted and a photoelectron image on a two-dimensional detector is reformed. This design represents a photoelectron microscope delivering photoelectron images for a set binding energy, and the lateral resolution will not depend on the azimuth angle.

The lateral resolution in imaging surface chemical analysis by XPS is mainly determined, depending on the principal design of instrument used, by either the shape of the intensity profile across the incident microfocused x-ray beam defining the resulting LSF or by the profile of the LSF characterizing the photoelectron microscope. The lateral resolution will also be influenced by the signal-to-noise (S/N) level achieved in the images or line-scans taken.[6,10] That means, in practical applications where major and trace elements are mapped, the lateral resolution achieved will be rather different, i.e., worse for the trace elements. Of course, the positional stability of the incident x-ray beam and the stability of the sample stage (vibrations and/or drifts) have also an impact on the achievable lateral resolution.

The methods available to characterize the lateral resolution of imaging XPS instruments in a comparable manner are

– the straight-edge method,
– the narrow-line method, and
– the grating method,

and the basic approaches are visualized in Fig. 2.

All three methods are standardized in ISO 18516:2019. In Secs. II B–II D, each of them is introduced in detail.

B. Straight-edge method

The well-known straight-edge method has advantages in that the measurement is rather simple. However, the meaning of this measurement for analysis is not always clear as noted by the

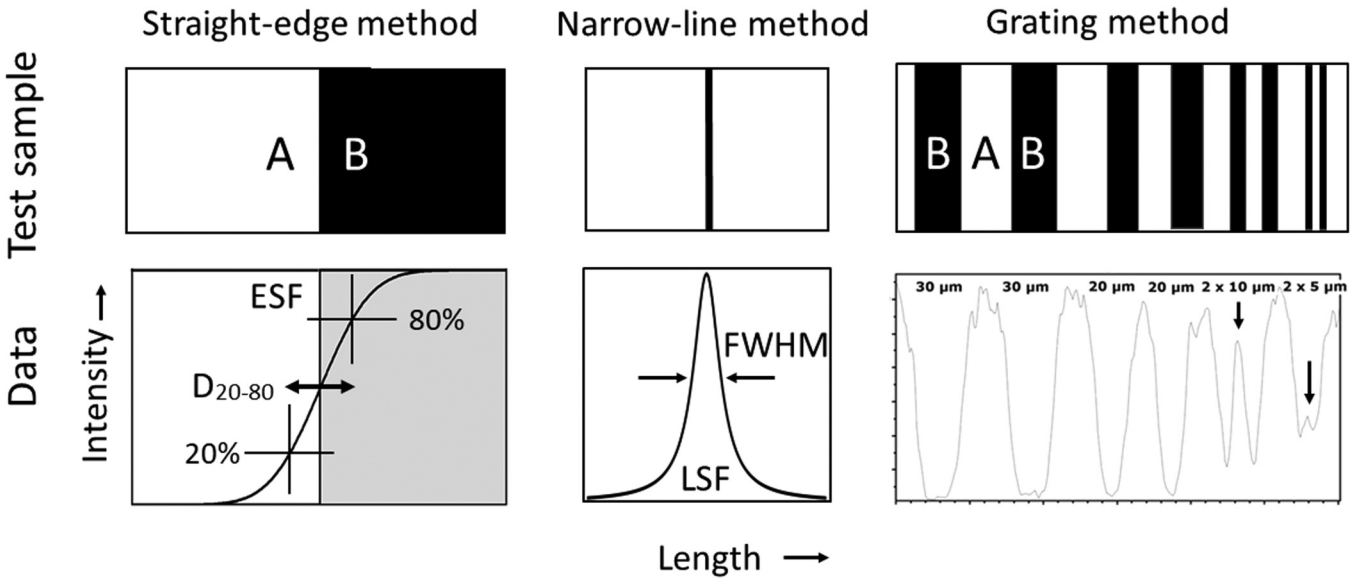

FIG. 2. Conceptual drawings to visualize the straight-edge, narrow-line, and grating methods used to express the lateral resolution of an imaging instrument. In all cases, the method-specific object patterns on the test specimen (Test sample) and the related signal distributions measured by the imaging instrument (Data) are shown. The test patterns are made from two different materials A and B selected to provide a contrast in the images. The straight-edge methods deliver the different $D_{x\text{-}(100-x)}$ parameters ($D_{20\text{-}80}$ shown, for example), the narrow-line method FWHM and shape of the LSF (here presented as a Lorentzian function showing substantial tails), and the grating method the lateral resolution expressed as the period of the narrowest grating resolved in the image. ISO 18516:2019 delivers a criterion that takes the noise in the image into account to decide whether a grating is resolved. In the respective line-scan shown for material A, an intense peak (arrow) reveals that the grating with the period 20 μm (bar widths 10 μm) is resolved. The result for the next grating made of 5 μm bars with only a little peak (arrow) does, not allow to conclude that the respective grating with period 10 μm is resolved.

authors of Ref. 12. Nowadays, it is still the most frequently used method to characterize the lateral resolution of imaging XPS instruments. To execute the method, a line-scan across or an image of a straight edge measured with appropriate sampling step width at a sufficiently high signal-to-noise ratio must be acquired. The test specimen must display a sharp chemical edge between material A and material B and appropriately long lengths of constant composition plateaus, to the left and right of the edge. The awareness for the latter requirement is somewhat limited in the community, which in turn is a reason for erroneous results in the scientific literature.

The straight-edge method delivers the parameter $D_{x\text{-}(100-x)}$, which characterizes the steepness of the sigmoidal ESF and is an indirect measure of the lateral resolution. The ESF is the result of a convolution of the edge represented by a box profile with the LSF. The LSF itself is characterizing the imaging instrument and determines its lateral resolution. For x, values as 12, 16, or 20 are commonly used. ISO 18516:2019 recommends using x = 12, i.e., the use of the 12% and 88% intensity of the maximum signal measured for the plateau characteristic of material A or B. Because a measurement of $D_{12\text{-}88}$ delivers larger values than for $D_{16\text{-}84}$ and $D_{20\text{-}80}$, i.e., an apparently inferior lateral resolution, vendors and many analysts prefer using the D parameters calculated using the higher x values.

One issue with the approach is that $D_{x\text{-}(100-x)}$ is a single distance parameter and not sufficient to fully characterize the shape of the ESF. Therefore, the character of $D_{x\text{-}(100-x)}$ remains ambiguous and the important question of what is the minimum spacing at which two features of an image can be recognized as distinct and separate cannot be answered from knowing that parameter only (cf. ISO/TR 19319:2013 and Ref. 9. A simulation shown in ISO/TR 19319:2013 reveals inherent ambiguity because the same D_{12-88} parameter can be obtained for different LSF shapes (Gaussian and Lorentzian). The lateral resolution, i.e., the ability to separate features, is shown to be substantially different for the different LSF shapes used in this simulation.

There is another issue with the $D_{x\text{-}(100-x)}$ parameters measured using a straight edge that has an impact on comparability and reproducibility. Knife edges, cleaved Si wafers, or mesh bars are often used as test specimens for executing the straight-edge method with XPS instruments where the best lateral resolution achieved is around 10 μm. In this case, material B is the vacuum. However, when using such a test specimen, the individual topography of the straight edge has an impact (via edge effects) on the resulting value of $D_{x\text{-}(100-x)}$. Those results will be inherently erroneous. As an example, Fig. 3 displays an Au 4f image of a finder-grid made from gold, acquired by a KRATOS Axis Ultra DLD instrument at BAM. Such grids are often used to determine the lateral resolution expressed by $D_{x\text{-}(100-x)}$ parameters. Basically, Fig. 3 shows how to make measurements that are not very meaningful because of different reasons. The first is that the width of the bars approaches the lateral resolution of the instrument tested and the $D_{x\text{-}(100-x)}$ parameters obtained are substantially underestimated

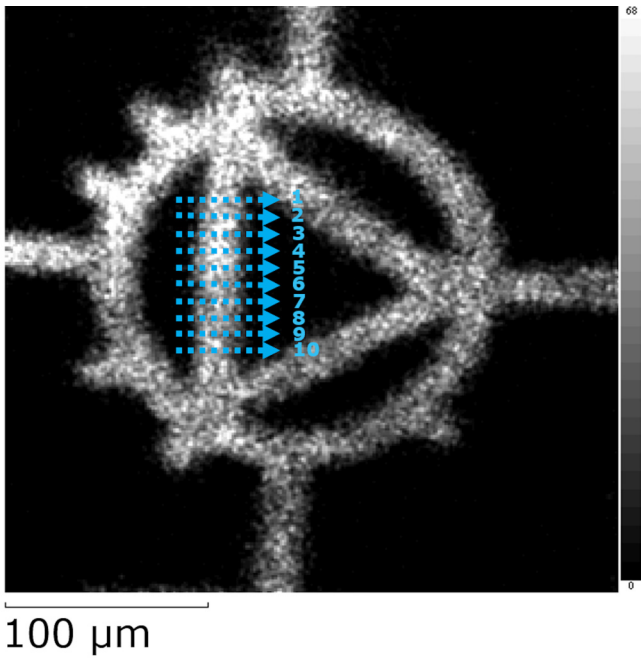

FIG. 3. Au 4f image of a gold finder-grid acquired by a KRATOS Axis Ultra XPS instrument displaying the loci of a set of ten parallel line-scans. The distance between the different line-scans was 5–10 μm. The width of the Au grid bar is 20 μm. Image acquisition parameters are as follows: excitation by monochromatized Al Ka x rays; lens mode set to FoV2, parallel imaging, iris aperture set to imaging in high-resolution mode, image taken at 83.6 eV binding energy using a pass energy of 160 eV, and image acquisition time: 60 s. For individual line-scans, see Fig. S3 (Ref. 21); for an optical microscopy image of the finder-grid, see Fig. S4 (Ref. 21).

(cf. Ref. 9). ISO/TR 19319:2013 delivers recommendations for the appropriate length of the material A plateau for running the straight-edge method. This length depends on the shape of the LSF. The LSF is, for the instruments using raster scanned x-ray beams, determined by the shape of the x-ray beam profile. For the photoelectron microscopes, the shape of the LSF is determined by the electron optical design. Common for both types of instruments is that the LSF typically displays wings, which have impact on the required plateau lengths. The FWHM of the LSF measured at the same instrument settings as used for the image shown Fig. 3 was estimated from imaging a narrow strip to be 12 μm [see next paragraph and Fig. S6 (Ref. 21)], and, therefore, a substantial underestimation of $D_{20\text{-}80}$ is expected because the required plateau length is much larger than the width of the grid bar providing the edge. As recommended in ISO/TR 19319:2013, the plateau length should be around two to three times the half width for a pure Gaussian shape of the LSF. For a Lorentzian shape, it must be much higher. The degree of underestimation of $D_{x\text{-}(100-x)}$ parameters caused by an insufficient plateau length is quantitatively discussed in Clause 4.35 in ISO/TR 19319:2013. When the straight-edge method is executed by using an Au 4f image taken by imaging the $200 \times 500\ \mu m^2$ box being part of the pattern on the ETH test sample [see Figs. S1 and S2 (Ref. 21)] at the same conditions as used to acquire the Au 4f finder-grid image in Fig. 3, a $D_{20\text{-}80}$ value of 16 μm is obtained [cf. Fig. S5 (Ref. 21)]. Because the plateau length used in this case was 120 μm, underestimation is not an issue anymore. This measurement delivers the true value for $D_{20\text{-}80}$.

TABLE I. $D_{20\text{-}80}$ parameters for ten line-scans as shown by arrows in Fig. 3. $D_{20\text{-}80}$ was automatically calculated by the KRATOS VISION Software 2.2.10 Rev 5. For individual line-scan profiles, see Fig. S3 (Ref. 21). For a comparison, the lateral resolution for the used instrument settings measured by the narrow-line method and expressed as the FWHM of the LSF is ~12 μm [cf. Fig. S6 (Ref. 21)].

Number of line-scan	$D_{20\text{-}80}$ (μm)
1	6.7
2	6.9
3	7.9
4	7.9
5	7.4
6	7.5
7	9.7
8	10.1
9	10.1
10	5.0
Mean	7.9
Standard Deviation	1.6

The second problem of the straight-edge method becomes obvious in an experiment addressing the impact of the geometry of the straight edge represented by the grid bar. We tested the variation of results for $D_{20\text{-}80}$ for a set of parallel line-scans across a bar of the finder-grid as shown in Fig. 3 and found (underestimated) values to vary in between 5 and 10 μm [cf. Table I and Fig. S3 (Ref. 21)]. Surely, this variation mostly relates to variations in the real topography of the imaged gold bar. The optical microscopy image of the grid bar shown in Fig. S4 (Ref. 21) supports this view. A recommendation concluded from the VAMAS A22 project was that comparability and reproducibility of results of the straight-edge method requires planar patterns on test specimens displaying the chemical edge. To be a useful test specimen for running the straight-edge method with high-end imaging XPS instruments, the height difference between structures of material A embedded in material B should be less than 50 nm.[6,13]

Finally, it must be mentioned that imaging of the Au finder-grid as shown in Fig. 3 has indeed its own value for the analyst. It is very useful to make quick adjustments to optimize any focal conditions of the used x-ray photoelectron microscope.

C. Narrow-line method

The narrow-line method is another method suitable for the characterization of the lateral resolution in imaging XPS. However, it has been rarely used so far. This is mainly caused by the lack of appropriate test specimens we are about to overcome. The narrow-line method can be viewed to be a variation of the method mentioned in Note 2 to the definition of *lateral resolution* in the terminology standard ISO 18115-1 (term 4.385). In that note, the

use of the "FWHM of the intensity distribution from a very small emitting point on the sample" is proposed. This intensity distribution represents the PSF. Because a narrow strip is a queue of many emitting points, the FWHM of the LSF can be measured in the respective experiment in shorter time at lower noise.

To execute the narrow-line method, a line-scan across or an image of a narrow strip measured with an appropriate sampling step width at a sufficiently high signal-to-noise ratio is acquired using a test specimen that displays a planar narrow strip of material A in material B. The strip width must be small (a delta line) in comparison to the expected lateral resolution of the instrument. As an estimate, the expected lateral resolution must be three to five times the width of the strip to get deviations from its real value below 5% (see ISO/TR 19319:2013, Clause 4.2.6). The method delivers the LSF, and the lateral resolution can be expressed as the parameter w_{LSF}, the FWHM of the LSF. It is important to know that the analysis of the measured profile principally delivers not only the FWHM but in addition the shape of the LSF. The shape of the measured LSF characterizes the profile of the x-ray beam used for instruments using raster scanning of an x-ray spot for imaging. For the photoelectron microscopes, the shape of the LSF is determined by their electron optical design. A conclusion here is that the method has potential to reveal the wings in the respective LSF profiles, which are important for a determination of the analysis area discussed later in Sec. III.

Participants in the VAMAS TWA 2 Project A22 tested the suitability of the planar test specimen prepared at the ETH shown in Figs. S1 and S2.[21] The specimen is displaying a planar 2 μm Ti strip in Au. This width is appropriate to execute the narrow-line method aiming on the measurement of FWHM and shape of the LSF characterizing imaging XPS instruments with lateral resolutions down to ~10 μm. In the supplementary material, LSF profiles are shown in Figs. S6 an S7.[21] In these very first results, the deviations of the measured LSF from a Gaussian profile and indications for wings are obvious for both instruments. After improvement of the noise level in the resulting LSF profiles, e.g., by summing up many line-scans retrieved from an image or much longer acquisition times for a line-scan acquisition, it can be expected that the LSF can be parameterized by fitting to meaningful models. A comparable determination of the shape of the LSF is on the horizon. For example, the FWHM of the LSF of the Axis Ultra instrument at BAM measured at the same instrument settings as given in the caption to Fig. 1 was estimated to be 12 μm (Fig. S6)[21] and that measured with the QuanteraSXM instrument at the ETH was estimated to be 15 μm (Fig. S7).[21]

D. Grating method

The grating method uses square-wave gratings, such as shown in Fig. 4, with different periods P and enables the determination of the lateral resolution in terms of the "minimum spacing at which two features of an image can be recognized as distinct and separate."[15] The use of gratings to determine the lateral resolution of an imaging instrument is an approach that is often applied in other communities using microscopy techniques. The period P here is a length set by the sum of the widths of a bar of material A and that of the neighbored bar of material B in an A-B-A grating. To name this length, the term "pitch" is also in use.

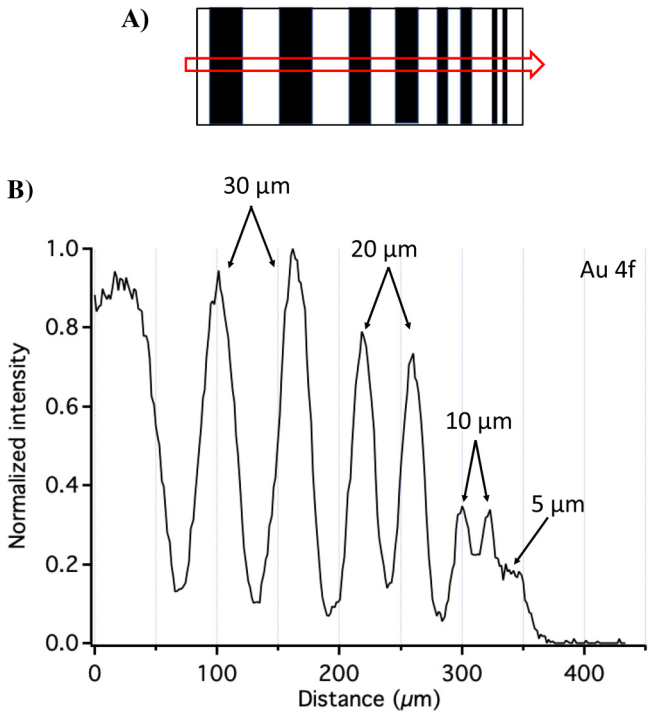

FIG. 4. (a) Principal layout of an earlier ETH prototype planar grating pattern displaying the line-scan direction (arrow) used for the determination of the lateral resolution by means of the grating method. Consecutive A-B-A gratings with Au bars (black, material A) in Ag (white, material B) having equal bar widths of 30, 20, 10, and 5 μm are available. The respective grating periods P are 60, 40, 20, and 10 μm. (b) Au 4f line-scan acquired by scanning a 9 μm (FWHM) x-ray spot across the gratings at normal incidence. A PHI Quantera SXM instrument at ETH was used. The FWHM of the x-ray beam profile was estimated by using the straight-edge method. A $D_{80\text{-}20}$ of 8.6 μm was measured in the line-scan direction and the one measured along the orthogonal direction was 8.3 μm. Therefore, the footprint of the x-ray beam should be circular, and azimuthal effects can be excluded. The complementary Ag 3d line-scan is shown in the supplementary material [Fig. S8 (Ref. 21)]. Line-scan acquisition parameters are as follows: excitation by monochromatized Al Kα x rays, analyzer pass energy set to 140 eV, energy step size 0.5 eV, 9 scans, and distance between analysis points 1.5 μm.

To run the grating method, either an image of a series of consecutive planar A-B-A gratings of material A in B or line-scans across that series of consecutive planar A-B-A gratings must be acquired using a planar test specimen that displays gratings that have periods narrower and wider than the expected lateral resolution. It is recommended to use gratings where the width of the respective A bar is equal to that of the B bar.[6] Data must be measured with an appropriate sampling step width to acquire enough data points even for the grating with the smallest period.[6,8] The grating method estimates the lateral resolution by using the known period P of the finest resolved grating.[8] ISO 18516:2019 delivers an objective criterion to decide whether a grating is resolved or not.

This criterion considers a signal measured across the width of bar B [depth of a dip in Fig. 4(b) or height of a peak in Fig. 5(b)] between the two material A bars in a line-scan in relation to the noise in the measured data. The noise in the image or line-scan has a strong impact on the lateral resolution achieved.[6,10]

The VAMAS TWA 2 Project A22 participants tested specimens displaying a pattern of consecutive A-B-A gratings with equal grating bar widths that were specifically designed for measuring the typical micrometer-scale lateral resolution of laboratory imaging XPS instruments, which is around 10 μm. The design of the pattern used was adopted from BAM L200,[16] a certified reference material (CRM) based on research undertaken earlier in the VAMAS TWA 2 Project A8. That project addressed procedures for the determination of lateral resolution of SIMS and AES instruments in the nanometer range.[17]

One advantage of the grating method is that there is no need for deeper knowledge of imaging theory, e.g., an insight into concepts behind PSF, ESF, and LSF and physical meanings of the parameters characterizing these functions. The performance of the imaging instrument is clearly expressed by the measured images or line-scans. The analyst immediately gets an answer regarding performance.

Examples of the determination of the lateral resolution of two different imaging XPS instruments estimated by the grating method are shown in Figs. 4 and 5. The used instruments represent both principal designs in use, one using x-ray raster scanning and the other the photoelectron microscope mode.

Figure 4 displays a line-scan of the planar A-B-A grating pattern on an earlier ETH prototype test specimen taken by an XPS instrument where a focused x-ray beam is scanned across the sample's surface to yield a line-scan. Looking at the Au 4f line-scan reveals that the A-B-A grating made of 10 μm bars (grating period P = 20 μm) is clearly resolved according to the resolution criterion in ISO 18516:2019 and that made of 5 μm bars (P = 10 μm) is not. So, it is demonstrated for the given instrument operation parameters that using an x-ray beam with an FWHM of ~9 μm (estimated as $D_{80\text{-}20}$ applying the straight-edge method) at normal incidence for imaging leads to a lateral resolution better than 20 μm but inferior to 10 μm. ISO 18516:2019 delivers an extra/interpolation procedure to estimate an assigned value in the interval 20–10 μm. The FWHM of the LSF measured under the same conditions is ~15 μm (cf. Fig. S7)[21] and consistent with the result of the grating method that an A-B-A grating with P = 20 μm can be resolved but the next with P = 10 μm cannot. Moreover, the analyst could use the depth of the Au 4f intensity dip between the Au bars measured for the grating with P = 20 μm as an arbitrary measure to control the lateral resolution of the instrument.

Figure 5 shows the use of an image of the planar A-B-A grating pattern on the ETH test specimen (Fig. S1)[21] taken by a Kratos Axis Ultra instrument used in the x-ray photoelectron microscope mode. Looking at the image and the line-scan immediately reveals that the grating made of 10 μm Ti bars (grating period P = 20 μm) is clearly resolved. The part of the line-scan crossing the grating made of 5 μm Ti bars (P = 10 μm) shows a small peak related to the Au bar (material B) between the Ti bars (material A), which is reproduced in more line-scans taken on other positions as shown in Fig. S9,[21] C to G, in the supplementary material. A standardized procedure and an objective criterion to decide whether

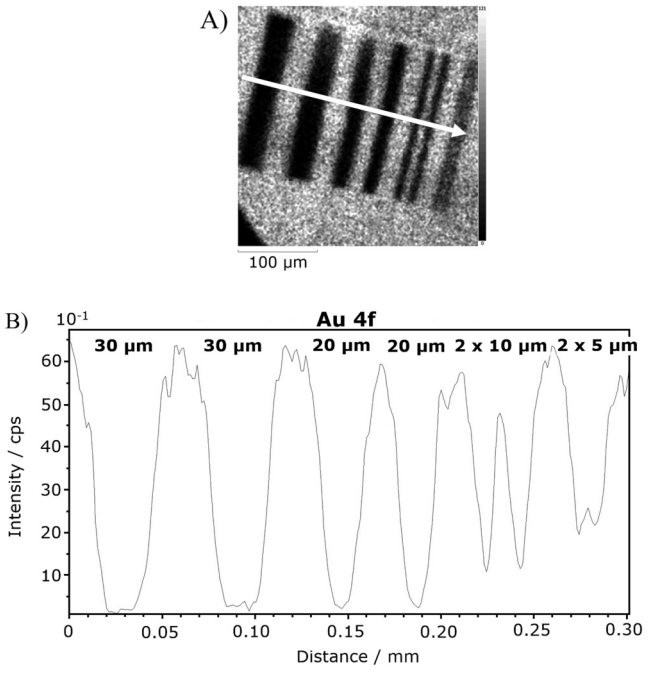

FIG. 5. (a) Au 4f image of the ETH test specimen [cf. Fig. S1 (Ref. 21)] used for an interlaboratory comparison in course of the VAMAS A22 project. The image was acquired by a KRATOS Axis Ultra DLD instrument at BAM. The test specimen displays consecutive planar A-B-A gratings with Ti (material A) bars having widths of 30, 20, 10, and 5 μm in Au (material B). A and B bars have always equal widths. Image acquisition parameters are as follows: excitation by monochromatized Al Kα x rays, lens mode set to FoV2, parallel imaging, iris aperture set to imaging in high-resolution mode, image taken at 83.6 eV binding energy using a pass energy of 160 eV, and image acquisition time: 300 s. The arrow shows the direction of the line-scan derived from that image and shown in (b). (b) Line-scan displaying the Au 4f intensity across the image of consecutive A-B-A gratings with Ti (material A) bars in Au (material B) retrieved by using the KRATOS VISION Software 2.2.10 Rev 5. The Ti bars are evident from the decaying Au 4f intensity and the Au bars in between by high Au 4f intensity. More line-scans retrieved from the Au 4f image in (a) are shown in the supplementary material [Fig. S9(C)–S9(G) (Ref. 21)] together with an Au 4f line-scan across an Au area below the grating, i.e., without Ti features. The latter one was taken to analyze the noise in the Au 4f signal.

such a peak is high enough in relation to the noise to conclude the grating is resolved is part of ISO 18516:2019. The standard also includes procedures to quantify the respective height of the peak and the noise in the image or line-scan. The height of the little peak in the Au 4f line-scan seen in Fig. 5(b) was determined to be $\sim 9 \times 10^{-1}$ cps adopting the approach standardized in ISO 18516:2019. (It must be noted that the standard considers a depth of the dip for a signal of material A in an A-B-A grating. In the given example, we are looking at a signal of material B and an inverted situation must be considered.) The standard deviation of the noise derived from the last line-scan shown in Fig. S9 (Ref. 21) was $\sim 5 \times 10^{-1}$ cps. These two numbers tell us that looking at a single Au 4f line-scan as displayed in Fig. 5(b) and following the criterion established in ISO 18516:2019, the grating with the bar

widths of 5 μm and a period P = 10 μm is not resolved. However, the lateral resolution established in the Au 4f image in Fig. 5(a) is substantially better than 20 μm, probably very close to 10 μm. This interpretation is underpinned by an estimated FWHM of 12 μm of the LSF measured for the same instrument operation parameters by applying the narrow-line method (Fig. S6).[21] However, cutting in half the noise level, e.g., by summing up many line-scans derived from the image in Fig 5(a), would almost satisfy the resolution criterion in ISO 18516:2019. The height of the peak in the Au 4f intensity between the Ti bars determined for the grating with the period P = 20 μm is, as in the former experiment using the Quantera instrument, useful as an arbitrary measure for a regular control of the lateral resolution of the instrument.

III. MEASUREMENT OF THE ANALYSIS AREA IN SMALL-SPOT (SMALL AREA) XPS

When running an XPS instrument in the small-spot (small area) mode, the question arises as to what contribution to the intensity originates from outside the nominal analysis area (cf. Fig. 6). The term *analysis area* is defined in the terminology standard ISO 18115:2015, term 4.9, see also Ref. 5. It is the "two-dimensional region of a sample surface measured in the plane of that surface from which the entire analytical signal or a specified percentage of the signal is detected." There are other terms in use to name the area selectivity of small-spot XPS, e.g., information area (ISO 18115:2015, term 4.245), field of view, acceptance area, sample area viewed by the analyzer (ISO 18115:2015, term 4.390), specimen area viewed by the analyzer,[12] quantitative lateral resolution,[18] and maybe more. Aiming on consistent terminology, the latter one should be avoided. Nevertheless, it points to a relation between analysis area and lateral resolution. A comprehensive discussion of that relationship was published by Baer and Shard aiming on a consistent terminology in XPS.[5] For instruments using a focused x-ray beam, the analysis area is assumed to be equal to the beam diameter. This diameter is typically approximated by using the straight-edge method, and the resulting $D_{20\text{-}80}$ is used as a measure of the FWHM of the intensity profile across the beam. To get a feeling for the deviation of this approximation from the true value, we refer to Note 2 to the definition of lateral resolution (term 4.385, ISO 18115-1) where it is mentioned that for a pure Gaussian beam profile, $D_{12\text{-}88}$ equals the FWHM of the LSF, w_{LSF}, i.e., that of the beam profile. In Table 4 of Clause 4.3.2 of ISO/TR 19319, the respective relations for a pure Lorentzian profile are given: $D_{12\text{-}88} = 0.715\ w_{LSF}$ and $D_{20\text{-}80} = 1.38\ w_{LSF}$. In summary, because the x-ray beam intensity profile is far away from a top-hat distribution, there is no beam diameter that simply equals the analysis area. To implement the definition of analysis area, it was proposed in Refs. 5, 12, and 18 to measure a specified percentage of signal intensity from an element outside a circular region of a known diameter. From that result, the intensity measured from inside the region can be calculated. 10% of the signal intensity originating from outside the analysis area is a reasonable number for practical applications.

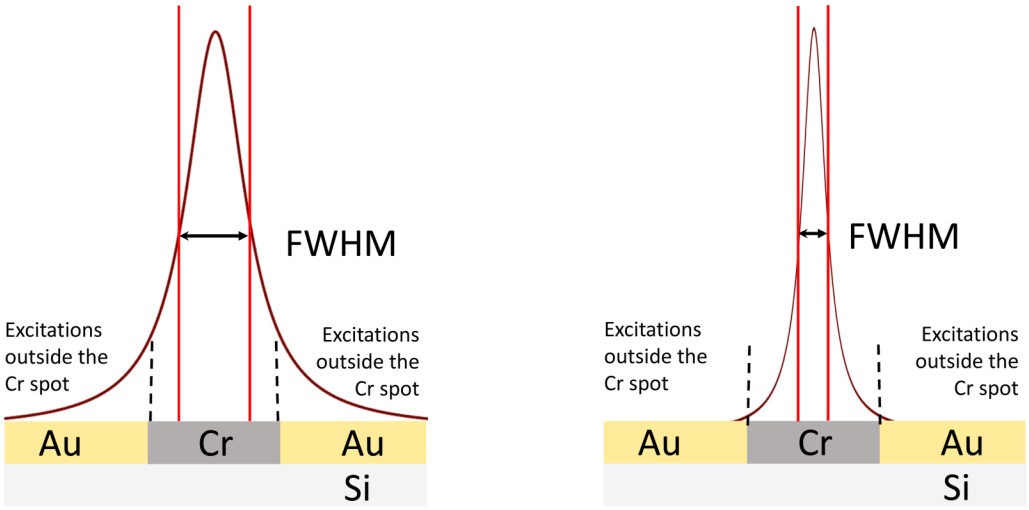

FIG. 6. Visualization of the problem of contributions to the intensity measured by small-spot XPS originating from outside the nominal analysis area. As an example, an instrument using a focused x-ray beam and the PTB test specimen [Fig. S10 (Ref. 21)] are used here. The x-ray beam is characterized by an intensity distribution represented by a nominal diameter, typically expressed as an FWHM approximated by a $D_{x\text{-}(100-x)}$ parameter measured by the straight-edge method, and wings. The authors of Ref. 12 discuss analytical profiles to model that intensity distribution. To preferentially acquire signal from inside the Cr spot of a certain diameter, a nominal diameter of the x-ray beam must be used, which is appropriately smaller. The cartoon on the right side visualizes this requirement and is realistic in a sense that the Cr spot size/x-ray beam FWHM ratio should be >3. The wings in the x-ray intensity distribution are the reason for intensity contributions originating from outside the nominal analysis area, here from the Au surroundings of the Cr spot. Figure 7 displays results of an approach developed to determine that intensity contribution for specific settings of an instrument. This approach enables us to select the nominal x-ray beam diameter necessary to minimize the contributions from outside the analyzed feature of a certain size down to a pre-set percentage.

For instruments where a focused x-ray beam is used, the nominal analysis area is typically specified by a measurement of the FWHM of the x-ray beam expressed as a D parameter measured by the straight-edge method. For an angle of incidence of the x-ray beam of $\Theta = 0°$, this FWHM is usually taken to represent the diameter of the footprint of the x-ray beam. However, this parameter does not inform on the wings in the x-ray intensity profile across the spot. With the help of the narrow-line method (cf. Sec. II C), it

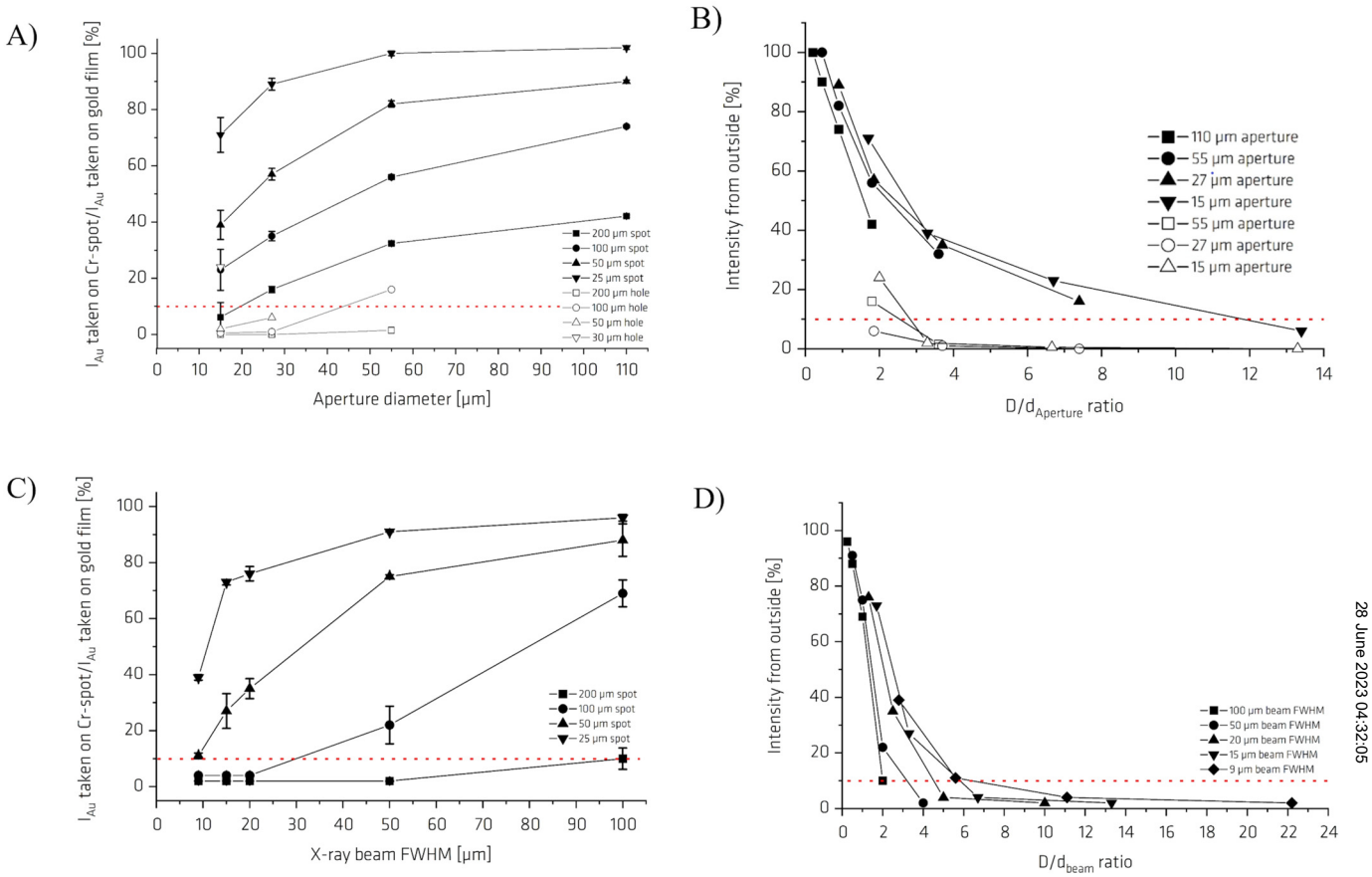

FIG. 7. Measurement of the ratio of the Au 4f intensity [I_{Au} on Cr spot (or hole)] measured after careful alignment of the center of a circular Cr spot in Au [on PTB's prototype test specimen, cf. Fig. S10 (Ref. 21)] or a hole in gold coated copper disks to the axis of the electron optical setup of Axis Ultra instruments or the focused x-ray beam in the QuanteraSXM instrument and the intensity (I_{Au} on Au film) measured on the Au film far away from the Cr spots of the PTB test specimen or holes in gold coated copper disks. The two smallest spots on the PTB test specimen were not used. They were included into the layout to cover future instrument developments. The dotted line always indicates the 10% level of the contribution from outside the addressed spot or hole. (a) Ratio I_{Au} on Cr spot/I_{Au} on Au film × 100% measured using a KRATOS AXIS Ultra DLD instrument at BAM utilizing monochromatized Al Kα excitation with the selected area aperture set to diameters $d_{Aperture}$ of 15, 27, 55, or 110 μm and using the FoV2 parallel imaging mode at 83.6 eV binding energy and pass energy set to 160 eV. The selected area aperture is part of lens column of the Axis instruments and determines the size of the analyzed area. Acquisition times were in the range of 200–500 s. Open symbols show results obtained by using an instrument in the demo lab of Kratos Analytical Ltd. utilizing a series of holes of different sizes (200, 100, 50, and 30 μm) in gold coated copper disks (National Aperture Inc., Salem, NH, USA) used as test specimens instead of the Cr spots on the PTB test specimen. This instrument was carefully tuned for high performance in small-spot XPS. Data reused from Hutton *et al.*, Quantitative Lateral Resolution of the Kratos AXIS Ultra and AXIS Nova XPS Instruments, AVS 55th International Symposium & Exhibition Poster (2008), see: https://www.kratos.com/application-areas/application-downloads/lateral-resolution-AXIS-instruments (accessed 12 August 2020). Copyright 2008, Kratos Analytical Ltd. (b) Presentation of Au 4f intensity ratio data shown in 4A vs the ratio of the Cr spot diameter D by the diameter of the selected area aperture $d_{Aperture}$ following Ref. 12. Open symbols show results obtained by using an instrument in the demo lab of Kratos Analytical Ltd. and holes in gold coated copper disks. Data reused from Hutton *et al.*, Quantitative Lateral Resolution of the Kratos AXIS Ultra and AXIS Nova XPS Instruments, AVS 55th International Symposium & Exhibition Poster (2008), see: https://www.kratos.com/application-areas/application-downloads/lateral-resolution-AXIS-instruments (accessed 12 August 2020). Copyright 2008, Kratos Analytical Ltd. (c) Ratio I_{Au} on Cr spot/I_{Au} on Au film × 100% measured using a PHI QuanteraSXM instrument with the nominal x-ray beam diameter (expressed as its FWHM determined by the straight-edge method) set to 9, 15, 20, 50, or 100 μm using Cr spots on the PTB test specimen. Measurement conditions are as follows: specimen sputtered by argon ions at 1 kV for 60 s, sputtered area 2 × 2 mm^2, excitation by monochromatized Al Kα x rays, and acquisition of Au4f photoelectrons at pass energy 112 eV in spectroscopy mode. (d) Presentation Au 4f intensity ratio data shown in 4C vs the ratio of the Cr spot diameter D by the nominal x-ray beam diameter (expressed as its FWHM) d_{beam} following Ref. 12.

should be principally possible to visualize and parameterize such wings. The wings are responsible for the unwanted intensity contribution from outside the nominal x-ray spot. Therefore, elemental analysis of the surface of a feature of interest of a size comparable or larger to that nominal x-ray spot size may also reveal elements that are only present outside the feature. Furthermore, there is a risk for false quantitative element analysis of the surface of a feature of interest for elements that are present both within and outside the feature of interest.

In the case of small-spot analysis by XPS instruments where a combination of a spot size aperture, an electron lens stack, and an iris for adjustment of the electron acceptance angle is used to limit the analysis area on the sample, usually the diameter of the spot size aperture is taken as a nominal value of the analysis area. Wing effects occur also in this case, and signal contributions from outside the specified spot must be considered. For the Kratos instruments, the authors of Ref. 19 showed that when the standard iris setting is changed by closing the iris, the profile is "sharpened" up and closer to a top-hat distribution. Moreover, using a smaller iris results in shorter tails at approximately the same analysis area.

This issue of contributions from outside the nominal analysis area in small-spot XPS is well known. One example from the semiconductor industry is the quantitative small-spot XPS analysis of unwanted (low surface concentration) contaminations of small features such as micrometer-scaled Al bond pads of microelectronic devices. Minor signal contributions from outside the bond pad generated by the wings mentioned above may lead to false quantitative analysis. An example from academia, the chemical composition of small contact areas on the surfaces of tribo-pairs[3,4] was already referred to in the Introduction.

In the year 2000, Baer and Engelhard[12] introduced an approach for qualifying the area selectivity in small-spot XPS analysis by using an indium tin oxide spot in a Cr layer on the MRS3 test specimen (GELLER MICRO ÅNALYTICAL LABORATORY, Topsfield, MA, USA). In 2008, Scheithauer[18] used a series of Pt apertures with diameters in the range of ~30 to ~600 μm to measure the intensity contribution from outside the analysis area. In 2014, partners of the EURAMET EMRP SurfChem project started to test specimens manufactured by the German National Metrology Institute, PTB, displaying planar patterns designed for a determination of the analysis area in small-spot XPS. This specimen displays two series of features (Cr squares and circular spots in Au) of different sizes available on one and the same test specimen (Fig. S10).[21] The experiences acquired were fed into the VAMAS A22 project, in which a new test specimen was developed by the ETH with planar patterns designed for a determination of analysis area in small-spot XPS [cf. Fig. S1 (Ref. 21) and Ref. 13]. Common to both test specimens is that they deliver sets of spots ranging from some 100 μm down to 5 μm made of element A (Cr, Ti, or Ag) embedded in a film made of element B, here Au. The specimens were prepared having steps at the transitions from element A to B with heights in the lower nanometer range.

Figure 7 displays results obtained with XPS instruments in the small-spot analysis mode representing the two different instrument designs mentioned above. The PTB test specimen shown in Fig. S10 (Ref. 21) was used with exceptions specified in the captions of Figs. 7(a) and 7(b). The approach is based on Au 4f intensity ratios calculated using the Au 4f intensity "I_{Au} on Cr spot" measured after careful alignment of the center of a selected circular Cr spot on the test specimen to the axis of the electron optical assembly of the electron spectrometer or the axis of the focused x-ray beam and the intensity "I_{Au} on Au film" measured on the Au film far away from the Cr spots. Datasets were acquired using a variety of Cr spot diameters D and selected area aperture sizes $d_{Aperture}$ or x-ray beam diameters d_{beam}, respectively.

The message taken from Figs. 7(a) and 7(b) is that when the Cr spot diameter is twice the selected area aperture size ($D/d_{Aperture} \sim 2$), we still have 40%–70% contributions from outside the spot. Even when using the smallest selected area aperture size and the largest spot diameter, we have some small contributions from outside the Cr spot. The uncertainty of measurement is high in the latter case because the Au 4f intensity is rather small. Comparison to benchmarking data obtained with a carefully tuned small-spot XPS instrument in Kratos' demo lab[19] reveals that readjustments of the instrument at BAM might be necessary to reduce contributions from outside the analysis area.

Figures 7(c) and 7(d) show that when the spot diameter is roughly twice the x-ray beam diameter expressed as the $D_{20\text{-}80}$ parameter ($D/d_{beam} = 2\text{–}3$), we may have 40% (9 μm beam diameter in 25 μm Cr spot) down to ~10% (100 μm beam diameter in 200 μm Cr spot) contributions from outside the Cr spot. Baer and Engelhard displayed the fraction of data collected from inside the spot (Fig. 2 in Ref. 12) and reported 60%–70% for $D/d_{beam} = 2\text{–}3$. These results are very similar to the data presented here.

The conclusion from the graphs displayed in Fig. 7 is that the diameter of the analyzed spot must be several times higher than the diameter expressed as the FWHM of the x-ray beam or the diameter of the selected area aperture to guarantee that a percentage of less than 10% of the measured intensity originates from outside the addressed Cr spot. It is recommended to analysts to measure graphs as shown in Fig. 7 to get control on the performance of their instrument used for small-spot analysis.

The approach displayed above which is inspired by those reported in Refs. 12 and 18 is in the focus of a new standardization activity launched by ISO TC 201 SC7, Electron Spectroscopies, in 2020. A new work item proposal on "Determination of analysis area in X-ray photoelectron spectroscopy, Auger electron spectroscopy and Secondary Ion Mass Spectrometry" will be submitted for ballot soon.

IV. SUMMARY AND RECOMMENDATIONS

Although the single number indications of instrument resolution are often requested from and provided by vendors, such numbers need to be carefully understood as they can be obtained in different ways and do not provide simple adequate information about some types of needed analysis. There are three well developed methods to determine the lateral resolution available.

The first one is the well-known straight-edge method delivering lateral resolution expressed as the $D_{x\text{-}(100-x)}$ parameter. Test samples are relatively easy to prepare, but a topography around the straight-edge is an issue when approaching lateral resolutions <10 μm. The number of the D parameter measured alone does not

tell anything about the LSF with its wings characterizing the imaging instrument at specific settings.

The second one is the narrow-line method, which is less commonly used because of a lack of test samples. This lack is subject to current efforts because of the growing need in the community. The advantage of the method is that it delivers information on the LSF, i.e., its FWHM and shape. The shape is visually apparent, and simple modeling can help identify tails.

The third one is the grating method, which is also less commonly used, again because of a lack of test samples. The use of test pattern displaying consecutive A-B-A gratings of varying grid element sizes allows quantification of the lateral resolution and modeling as well as visual indication of imaging conditions. The advantage of the grating method is that there is no need for deeper knowledge of imaging theory. The performance of the imaging instrument is clearly expressed by the measured images or line-scans.

The type of resolution needed for the identification chemical differences in a small area is different than the question of how much signal comes from outside of an area when the analyst needs information only from a specified small area. To get 90% of the XPS signal originating from a small area, it needs to be more than three times larger than the measured instrument spatial resolution, expressed as the x-ray beam FWHM or the specimen area accepted by an analyzer, usually defined by an area selective aperture. The needed ratio will also depend on specific instrument type setup and conditions. If a high degree of area selectivity must be guaranteed, the use of test samples to validate conditions will be needed.

Specific recommendations for an achievement of comparability and reproducibility in measurements of the lateral resolution and contributions from outside the nominal analysis area derived from experimental results reported in Secs. II and III are the following:

- Because topography effects may adulterate results for the lateral resolution of imaging instruments in the lower micrometer range, test specimens must be planar, preferentially on a lower nanometer scale. International experts participating in the VAMAS A22 or EMRP SurfChem projects had a strong preference for the use of gold as the basic element of such test specimens, either to form the patterns or to host them. Both aspects for a design of test specimens are addressed by the prototype test specimen used for the measurements reported in this paper. It is planned to commercialize the all-in-one test specimen by ETH Zurich and the PTB test specimen displaying features for the determination of the intensity originating from outside the analysis area as well. The design of latter one will be changed in a way that all features are organized in one line. Furthermore, it is envisaged to implement ISO 18516 procedures as image data analysis tools in the CASAXPS software package.[20]
- Lateral resolution can be expressed by a $D_{x\text{-}(100-x)}$ parameter determined by the straight-edge method. Because the ESF cannot be fully described by the single parameter D, it must remain ambiguous because it *a priori* tells nothing about the shape (e.g., Gaussian, Lorentzian, mixture of both, etc.) of the line spread function behind. The shape of the line spread function has a strong effect on the plateau length left and right from the edge necessary to determine a correct value for the parameter D of the edge spread function. Specifically, for a distinct Lorentzian character (wide wings) of the line spread function, we need rather long plateaus to avoid underestimations of D.
- Lateral resolution can be expressed by the parameter w_{LSF}, the FWHM of the LSF, determined by the narrow-line method. A full determination of the line spread function is rather useful because it characterizes also the shape of the x-ray beam profile in raster scanning instruments or the response of a photoelectron microscope. It is useful for an identification of wide wings in LSF profiles. In a wider sense, the line spread function represents here a type of spectrometer function characterizing the imaging instrument and determining the resolution achieved in an image.
- Lateral resolution can be estimated by running the grating method to be the period of the smallest resolved A-B-A grating. In that case, lateral resolution is no more delivered by an abstract parameter but easy to understand as the minimum spacing at which two features of an image can be recognized as distinct and separate. For a decision whether a grating is resolved or not, ISO 18516:2019 delivers a criterion that takes the noise in an image into account.
- To deliver evidence that most of the measured photoelectron intensities (expressed as a certain pre-set percentage) originate from the surface of a feature of interest in small-spot/small area XPS, a measurement of the contributions from outside the nominal analysis area is required. These contributions originate from the wings in the intensity profile across the x-ray beam used or the capability to limit the analyzed area by electron optical assemblies. It is recommended to produce graphs characterizing the instrument's performance like those displayed in Fig. 7.
- There is a growing need in the community for imaging and small analysis area measurements in XPS. However, appropriate reference materials are still subject to current efforts and some relevant reference materials are not yet readily available.

We can conclude that means necessary to establish comparability and reproducibility in imaging and small-spot XPS are developed, but the awareness in the community needs further improvement. Appropriate test specimens for the determination of the lateral resolution and the contributions from outside the analysis area were tested during the VAMAS A22 project and are about to be commercialized. A supporting ISO standard is available for measuring the lateral resolution in surface chemical analysis by imaging SIMS, AES, and XPS instruments and another one addressing the measurement of the contributions from outside the analysis area is in preparation.

Test reports and scientific publications making substantial use of results of imaging and small-spot/small area XPS should always contain a proof on how the required measurement capability was established. Guidance on how to report the measurements undertaken to determine the lateral resolution for all three measurement methods outlined in Sec. II of this paper is given in the standard ISO 18516:2019. The future ISO standard addressing the measurement of the analysis area will also contain a clause with guidance for reporting results.

Furthermore, a regular check for appropriate XPS instrument calibration and specification of its performance in imaging or

small-spot (small area) XPS modes should be part of the reviewing process of journals publishing papers reporting such XPS data.

The experimental data presented in this paper have been provided to illustrate approaches that can be used to obtain a comparable and reproducible determination of the lateral resolution and the contributions from outside the nominal analysis area in imaging and small-spot XPS, respectively. The measurements were collected from specific instruments at specific times and not necessarily represent optimized instrument setups, and they are not from the most recent instrument generation. As demonstrated in the paper, consistent systematic approaches are required to collect data that would enable comparison of instrument performance from different vendors, which was not the intent here. The instruments used in this study show that the approaches presented work well for x-ray raster scanning instruments and x-ray photoelectron spectrometers/microscopes in their different modes. It is anticipated that these approaches will provide useful information and the exciting advances in instrument performance continue.

ACKNOWLEDGMENTS

Many thanks are due to D. Baer (PNNL, Richland, Washington) for reading the draft resulting in very helpful comments, S. Hutton and A. Roberts (Kratos Analytical Ltd., Manchester, UK) for communication about technical details of the design of Kratos XPS instruments and the permission to use data presented in Figs. 7(a) and 7(b), and, last but not least, one of the referees who made excellent proposals for making the paper more didactic.

REFERENCES

[1]D. R. Baer and I. S. Gilmore, J. Vac. Sci. Technol. A **36**, 068502 (2018).
[2]D. R. Baer *et al.*, J. Vac. Sci. Technol. A **37**, 031401 (2019).
[3]M. Eglin, A. Rossi, and N. D. Spencer, Tribol. Lett. **15**, 199 (2003).
[4]A. Rossi, M. Eglin, F. M. Piras, K. Matsumoto, and N. D. Spencer, Wear **256**, 578 (2004).
[5]D. R. Baer and A. G. Shard, J. Vac. Sci. Technol. A **38**, 031203 (2020).
[6]ISO, *ISO/TR 19319:2013, Surface Chemical Analysis—Fundamental Approaches to Determination of Lateral Resolution and Sharpness in Beam-Based Methods* (ISO, Geneva, 2013).
[7]M. Senoner and W. E. S. Unger, Surf. Interface Anal. **45**, 1313 (2013).
[8]ISO, *ISO 18516:2019, Surface Chemical Analysis—Determination of Lateral Resolution and Sharpness in Beam-Based Methods With a Range From Nanometres to Micrometres* (ISO, Geneva, 2019).
[9]W. E. S. Unger, M. Senoner, Th. Wirth, S. Bütefisch, and I. Busch, J. Surf. Anal. **24**, 123 (2017).
[10]M. Senoner, T. Wirth, and W. E. S. Unger, J. Anal. At. Spectrom. **25**, 1440 (2010).
[11]ASTM International, *ASTM E1217—11, Standard Practice for Determination of the Specimen Area Contributing to the Detected Signal in Auger Electron Spectrometers and Some X-Ray Photoelectron Spectrometers* (ASTM International, West Conshohocken, PA, 2019).
[12]D. R. Baer and M. H. Engelhard, Surf. Interface Anal. **29**, 766 (2000).
[13]C. Passiu, A. Rossi, L. Bernard, D. Paul, J. Hammond, W. E. S. Unger, N. V. Venkataraman, and N. D. Spencer, Langmuir **33**, 5657 (2017).
[14]W. E. S. Unger, J. Vac. Sci. Technol. A **38**, 021201 (2020).
[15]ISO, *ISO 22493, 2008 Microbeam Analysis—Scanning Electron Microscopy—Vocabulary* (ISO, Geneva, 2008).
[16]M. Senoner *et al.*, Anal. Bioanal. Chem. **407**, 3211 (2015).
[17]M. Senoner and W. Unger, Surf. Interface Anal. **39**, 16 (2007).
[18]U. Scheithauer, Surf. Interface Anal. **40**, 706 (2008).
[19]S. Hutton, C. Blomfield, and G. Mishra, *Quantitative Lateral Resolution of the Kratos AXIS Ultra and AXIS Nova XPS Instruments, AVS 55th International Symposium & Exhibition Poster* (2008), see: https://www.kratos.com/application-areas/application-downloads/lateral-resolution-AXIS-instruments (accessed 12 August 2020).
[20]See: http://www.casaxps.com/ (accessed 10 June 2020).
[21]See supplementary material at http://dx.doi.org/10.1116/6.0000398 for the layout of ETH and PTB prototype test specimens used in the VAMAS A22 project for a determination of lateral resolution and contributions from outside the analysis area, respectively; all Au 4f line scans across an Au bar in a gold finder-grid image and the 500 μm × 200 μm Ti box on the ETH test specimen using the KRATOS Axis Ultra DLD XPS instrument (straight-edge method); Au 4f line scans across the 2 μm Ti strip on the ETH prototype test specimen acquired using both instruments (narrow-line method); all the different Au 4f line scans across the consecutive gratings of Ti bars in Au on the ETH test specimen acquired using the KRATOS Axis Ultra DLD XPS instrument (grating method).